Acta Cryst. (1952). **5**, 168

A Study of Cold-Worked Aluminium by an X-ray Micro-Beam Technique. II. Measurement of Shapes of Spots

BY P. B. HIRSCH

Crystallographic Laboratory, Cavendish Laboratory, Cambridge, England

(*Received* 16 *May* 1951 *and in revised form* 17 *June* 1951)

A method is described for obtaining from the shapes of the spots on spotty-ring photographs approximate values of the physical broadenings of the reflexions. The method is used to determine the broadenings of the reflexions from particles of specimens of cold-rolled aluminium examined by the micro-beam technique. It is found that the physical broadenings decrease with time after rolling. The general application of the method to spotty-ring and Laue photographs from stationary specimens is discussed.

1. Introduction

In the recent micro-beam study of the structure of cold-worked aluminium, it was found that spotty back-reflexion rings could be obtained from this material even after heavy deformation. The determination of particle size and misorientations has been described in a previous paper (Hirsch & Kellar, 1952). This paper deals with the determination of the physical broadenings of the reflexions from the shapes of the spots, with a view to obtaining an estimate of the perfection of the particles.

The intensity distribution across a continuous Debye–Scherrer line depends both on instrumental and physical factors. In order to determine, for example, the physical line breadths it is necessary to correct for the instrumental broadening (e.g. Jones, 1938). In a similar manner, the shapes of the spots on an X-ray photograph depend on instrumental constants such as the divergence of the X-ray beam and the wavelength spread of the radiation, and on the shape and distortion of the diffracting particles. As in the case of continuous diffraction lines, it is necessary to eliminate the instrumental factors, and this paper describes a method for obtaining the physical broadenings.

The method is applied to the micro-beam photographs of cold-worked aluminium. The results are interpreted in terms of particle shape and distortion in a later paper.

THEORY OF METHOD

2. The angular broadening

The size of the spot on the film depends on the cross-section of the particle in the beam and on the divergence of the beam reflected from the crystal. If the cross-section of the particle is negligible, or if the specimen–film distance is increased sufficiently, the shape of the spot on the film is determined almost completely by the angular breadth of the reflexion from the crystal, which can be treated as a point. This angular broadening will be considered in the following sections.

Both a radial (s_R) and a tangential (s_T) width of the spots can be distinguished normal and tangential to the diffraction ring respectively. If A_R and A_T are the corresponding angular breadths, it follows from simple geometry that

$$s_T = \frac{R_0}{|\cos 2\theta|} A_T , \qquad (1)$$

and

$$s_R = \frac{R_0}{\cos^2 2\theta} A_R , \qquad (2)$$

where R_0 is the specimen–film distance and θ is the Bragg angle.

3. Reflecting sphere construction (Fig. 1)

The angular breadths of reflexion can be discussed conveniently in terms of the reciprocal lattice (origin O) and the reflecting sphere (centre C, radius $1/\lambda$). To apply the construction to the reflexion from stationary

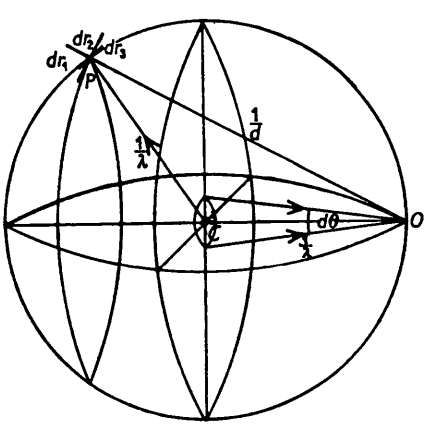

Fig. 1. Reflecting sphere construction for stationary crystal.

crystals, it is necessary to represent the divergence of the beam, the wave-length spread of the radiation, the shape and the distortion of the particle. The shape and distortion of a particle are represented in reciprocal space by a volume associated with the reciprocal point, P, of the reflexion (the interference function) (James, 1948, chap. 10). For simplicity it may be assumed that the shape of the interference function is a rectangular parallelopiped with lengths dr_1, dr_2, dr_3 in directions OP, perpendicular to OP in the plane OPC, and perpendicular to the plane OPC respectively. For a given orientation of a stationary crystal, OP is fixed in direction.

A divergence, $d\theta$, is represented by a cone of semi-angle $\frac{1}{2}d\theta$ with axis OC and apex O, and a wave-length spread by a range of values of the radius of the reflecting sphere (OC or CP). Then, if OC' is any component of the divergent X-ray beam of wave-length λ', and OP' is any particular direction in the reciprocal lattice corresponding to a point P' within the volume associated with the reciprocal point P, the condition of diffraction is that $OC'=C'P'=1/\lambda'$.

The broadenings calculated are the angles between extreme rays. The breadths measured experimentally will approximate to the half-peak widths of the distribution curves of intensity of the reflexions. No attempt has been made to calculate the distribution of intensity expected from the simple shape of interference function assumed. Further, the actual distribution of intensity will depend on the actual distribution of the interference function around the reciprocal point. It is clear, therefore, that the values of the physical broadenings, obtained by applying the formulae (given in the following sections) to the experimentally observed shapes of the spots, can be regarded as orders of magnitude only.

A further assumption made in the calculations is that the particles are in the best reflecting positions. However, reflexions should occur with breadths between zero and a maximum; in practice, a study of the distribution of measured spot lengths shows that only the larger spots are measured, and therefore this assumption is partly satisfied (Hirsch, 1950).

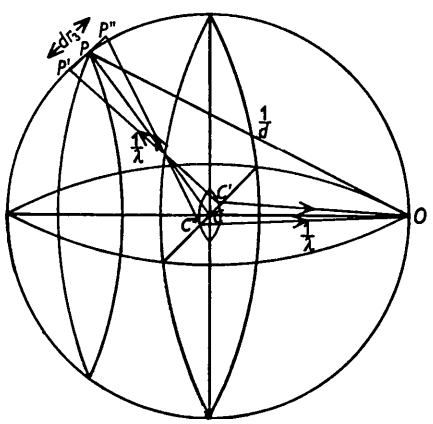

Fig. 2. Tangential broadening.

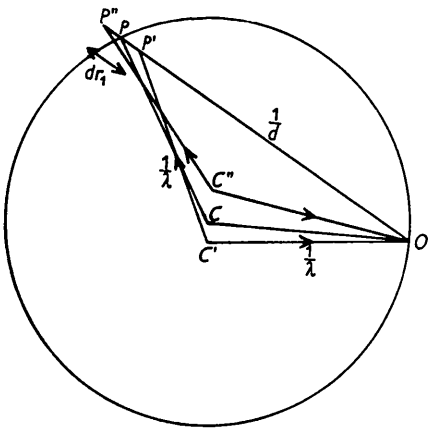

Fig. 3. Definition of $d\varphi_1$.

4. Tangential broadenings (Fig. 2)

The elements dr_1 and dr_2 cause broadening in the plane OPC only; the tangential broadening is due entirely to dr_3 and $d\theta$. It follows from geometry (Hirsch, 1950) that $A_T = d\theta+\lambda dr_3$.

If $d\varphi_3$ is the angle subtended by dr_3 at O,

$$d\varphi_3 = \frac{\lambda dr_3}{2\sin\theta}, \tag{3}$$

and

$$A_T = d\theta+2\sin\theta d\varphi_3. \tag{4}$$

5. Radial broadening

This presents a more difficult problem than the tangential broadening. Several different cases have to be discussed, depending on the relative magnitude of the factors contributing to the broadening. The variables involved are the divergence of the X-ray beam, the wavelength spread, $d\lambda$, and the physical broadening expressed by dr_1, dr_2. To find the radial broadening only a section through C, O and P need be considered.

It is convenient to define two angular ranges ($d\varphi_1$, $d\varphi_2$) which are equal, respectively, to the possible angular breadths of reflexion of a monochromatic beam, of infinite divergence, due to dr_1 and dr_2. Their relation to dr_1, dr_2, respectively, can be obtained from Figs. 3 and 4. $d\varphi_1$ is equal to the angle between $C'P'$ and $C''P''$, obtained by constructing isosceles triangles with equal sides on OP' and OP'', respectively, as base. It follows that

$$d\varphi_1 = \frac{\lambda dr_1}{2\cos\theta}. \tag{5}$$

The angle $d\varphi_2$ is equal to the angle between $C'P'$ and $C''P''$, obtained by rotating triangle OCP around O. Then

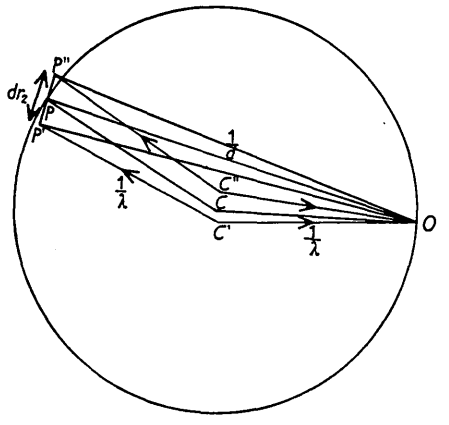

Fig. 4. Definition of $d\varphi_2$.

$$d\varphi_2 = \frac{\lambda dr_2}{2\sin\theta}. \tag{6}$$

It is also necessary to define an angle $d\alpha$ giving the broadening due to the wave-length spread $d\lambda$; then

$$d\alpha = \frac{d\lambda}{\lambda}\tan\theta. \tag{7}$$

The derivation of the physical broadenings in terms of $d\varphi_1$, $d\varphi_2$ and $d\alpha$ is described elsewhere (Hirsch, 1950). The results are given in Table 1.

Table 1. *Radial breadths*

		$d\theta$	A_R	
$d\varphi_1+d\alpha > d\varphi_2$	$<(d\varphi_1+d\alpha)-d\varphi_2$	$2d\varphi_2+d\theta$	(8)
	$>(d\varphi_1+d\alpha)-d\varphi_2$	$d\varphi_1+d\varphi_2+d\alpha$	(9)
$d\varphi_1+d\alpha < d\varphi_2$	$<d\varphi_2-(d\varphi_1+d\alpha)$	$2(d\varphi_1+d\alpha)+d\theta$	(10)
	$>d\varphi_2-(d\varphi_1+d\alpha)$	$d\varphi_1+d\varphi_2+d\alpha$	(11)

Two cases may now be distinguished. For Laue spots, i.e. spots due to white radiation, $d\lambda$ and, therefore, $d\alpha$ are very large. Hence equation (8) is applicable, so that for Laue spots (e.g. asterism streaks)

$$A_R = 2d\varphi_2+d\theta. \tag{12}$$

The tangential broadening is, of course, given by (4). It follows that under any conditions, A_R and A_T for Laue spots give particular extensions of the interference function at the reciprocal lattice point. The extension dr_1 cannot be determined, and hence no direct estimate of a possible range of lattice spacings (or strains) can be obtained from asterism streaks.

In the present series of micro-beam experiments only characteristic-radiation spots have been examined. For these $d\lambda$ is limited and equal to the wave-length spread of the emission lines. This, however, can have an appreciable effect in the back-reflexion region. For Cu $K\alpha$ radiation $d\lambda = 0{\cdot}00058$ Å (Compton & Allison, 1935, chap. 8). Hence, for the 422 reflexion from aluminium ($\theta = 69{\cdot}1°$), $d\alpha = 10^{-3}$ radians. This is appreciable compared with the breadths of the reflexions. Several of the cases considered above may be applicable. In order to obtain radial breadths which can be interpreted easily, the divergence should be large compared with the spread of reflexion. In that case A_R can be determined unambiguously, and is equal to $d\varphi_1+d\varphi_2+d\alpha$.* However, it may be possible to use smaller divergences, and to apply one or other of the formulae quoted. Although the relative magnitudes of $d\theta$, $d\varphi_1$, $d\varphi_2$ are not known, the number of possibilities is small since the results must be self-consistent.

6. Relative magnitudes of broadenings

In back-reflexion work, if $d\varphi_2$ and $d\varphi_3$ are averaged around the ring, the mean values of dr_2 and dr_3 should be equal, for an extension dr_2 becomes an extension dr_3 at 90° along the ring. Hence, if the breadths are averaged around the ring, $d\varphi_2 \doteqdot d\varphi_3$.

If in the averaging process the average interference function becomes spherically symmetrical, $dr_1 = dr_2$. Hence, from (5) and (6), $d\varphi_1/d\varphi_2 = \tan\theta$. In the back-reflexion region $\tan\theta$ is large, and hence the possible broadening due to dr_1 is greater than that due to dr_2. Conversely, if $d\varphi_1/d\varphi_2 \sim \tan\theta$, the average interference function is approximately spherically symmetrical.

7. Application

Specimens of heavily cold-worked spectroscopically pure aluminium were examined; the particle size of these specimens determined from the number of spots around the rings was about 2 μ. The spots (diameter 50–100 μ) were much larger and therefore gave the angular breadths of the reflexions. The films were examined under a microscope with calibrated eyepiece.

To test the theory, a series of X-ray photographs with different divergences were taken of a heavily rolled and subsequently recovered specimen. The tangential and radial spot widths were measured and averaged around the ring. The results obtained were in agreement with the theory (for further details see Hirsch, 1950), and the average reciprocal volume was found to be nearly spherically symmetrical. All other broadenings have been deduced by direct application of the formulae to the broadenings observed on one photograph, as follows:

A photograph of a specimen examined immediately after heavy rolling gave these results:

* It should be noted here that the angular range in the incident beam which contributes to the reflexion is also equal to $d\varphi_1+d\varphi_2+d\alpha$. This expression is equal to Δ, required for the calculation of the probability of reflexion of a particle (see Hirsch & Kellar, 1952, §§ 6, 7).

$$d\theta = 1{\cdot}6\times10^{-3} \text{ radians},$$
$$s_T R_0 = 6{\cdot}9\times10^{-3} \text{ radians},$$
$$s_R/R_0 = 8{\cdot}4\times10^{-3} \text{ radians}.$$

Tangential broadening. Using equations (1) and (4),

$$d\varphi_3 (\doteq d\varphi_2) = 1{\cdot}9\times10^{-3} \text{ radians}.$$

Radial broadening. Suppose first that

$$d\varphi_1 + d\alpha < d\varphi_2;$$

then $$d\varphi_1 < 9\times10^{-4} \text{ radians};$$

since $d\theta = 1{\cdot}6\times10^{-3}$, equation (11) applies, and hence

$$d\varphi_1 = 1{\cdot}8\times10^{-3}$$

which is not consistent with the previous condition for $d\varphi_1$. Therefore, in this case,

$$d\varphi_2 < d\varphi_1 + d\alpha.$$

Suppose now $$d\theta < d\varphi_1 + d\alpha - d\varphi_2;$$

applying (8) we obtain $d\varphi_2 = 1{\cdot}5\times10^{-3}$.
This agrees well with the value of $d\varphi_2$ expected from the tangential breadths. Also, it follows that for self consistency,

$$d\varphi_1 > d\theta + d\varphi_2 - d\alpha$$
$$> 2{\cdot}5\times10^{-3} > d\varphi_2.$$

This is a possible interpretation.

Suppose next

$$d\theta > d\varphi_1 + d\alpha - d\varphi_2;$$

applying equation (9), $d\varphi_1 = 1{\cdot}8\times10^{-3}$.

Further, $d\varphi_1 + d\alpha - d\varphi_2 = 9\times10^{-4} < d\theta$, and therefore the results are self consistent. However, in this case $d\varphi_1 \sim d\varphi_2$, whereas it is more likely that on averaging $d\varphi_1 > d\varphi_2$.

Hence the first of the two interpretations is preferred, i.e.

$$d\varphi_2 \sim 1{\cdot}5\times10^{-3},$$
$$d\varphi_3 \sim 1{\cdot}9\times10^{-3},$$
$$d\varphi_1 > 2{\cdot}5\times10^{-3}.$$

All the other results have been similarly deduced, (Hirsch, 1950).

RESULTS

8. Broadenings as a function of deformation

For small deformations the broadenings (particularly s_T) cannot be measured accurately because of the poor resolution of the spots. No attempt has been made to deduce the physical breadths from the results, but the radial breadths shown in Table 2 indicate that even for small deformations the broadening is considerable. The value of s_R/R_0 for the undeformed material is given for reference, though a large part of the size of the spot is due to the cross-section of the particles.

Table 2. *Radial broadenings as function of deformation*
(Specimens examined immediately after rolling)

Reduction (%)	$t(\mu)$	s_R/R_0	$d\theta$ (radians)
0	20	58×10^{-4}	2×10^{-3}
1·3	4	88	2
3	5	74	2·3
8	2	78	2
57	2	84	1·6

For impure aluminium the broadenings were even more difficult to measure, but were found to be of the same order as those for the spectroscopically pure material.

9. Broadenings as a function of time after rolling

Specimens of heavily cold-rolled spectroscopically pure aluminium were used. The results are shown in Table 3.

These (and other) results show quite clearly that the average broadenings decrease with time after rolling. This corresponds to the decrease in line-broadening accompanying recovery.

10. Spot shapes

So far only average spot lengths have been considered. As expected, the results are consistent with an approximately spherically symmetrical average interference function. It does not follow, however, that the distribution around the reciprocal point for a reflexion from a particular particle is spherically symmetrical. In fact, the shapes of individual spots indicate that the interference functions individually are asymmetric. The arcs of many spots are neither radial nor tangential to the ring (see Hirsch & Kellar, 1952, Fig. 6(*b*)). The variation of the directions of the arcs of the spots shows that the effect is not due to the linear shape of the focus, but is inherent in the material.

The tangential and radial breadths of typical spots were measured at various points around the ring, and, using the values of $d\theta$ appropriate at these points, some or all of the physical breadths were determined. The results showed that the breadths of typical spots

Table 3. *Broadenings as a function of time after rolling*
(All angles in radians)

Time of examination after rolling	s_T/R_0	s_R/R_0	$d\theta$	$d\varphi_1$	$d\varphi_2$	$d\varphi$
2 days	69	84	$1{\cdot}6\times10^{-3}$	$> 2{\cdot}5\times10^{-3}$	$1{\cdot}5\times10^{-3}$	$1{\cdot}9\times10^{-3}$
4 months	52	76	$2{\cdot}4\times10^{-3}$	$\sim 2{\cdot}6\times10^{-3}$	9×10^{-4}	8×10^{-4}
1 year	41	51	$2{\cdot}4\times10^{-3}$	$1{\cdot}4\times10^{-3}$	4×10^{-4}	4×10^{-4}

did not generally differ from the average breadths by more than a factor of ~ 2, with the possible exception of some spots of the recovered material. In general, therefore, the asymmetry of the interference function does not seem to be very pronounced (Hirsch, 1950).

11. Background

A characteristic feature of the micro-beam photographs of rolled aluminium is the background between spots. For slightly deformed material the background and spots form an arc of continuously varying radius. It follows that the background between spots is due to boundary regions between particles (see Hirsch & Kellar, 1952). For the heavily rolled material neighbouring spots are sometimes joined continuously by background, thus indicating that the particles are neighbours and that the background is due to the boundary region between them. After recovery, this background largely disappears. This diffuse nature of the background suggests that the boundary region consists of highly distorted material.

12. Conclusions

The method described in this paper enables the determination of approximate values (to perhaps within a factor of 2) of the breadths of the interference function in reciprocal space from the shapes of the spots. It should be emphasised that this method can be applied to any spotty-ring photograph from stationary specimens (not only to micro-beam photographs), provided that the spots on the photographs are large compared with the dimensions of the diffracting crystals. This condition can usually be satisfied by choosing a sufficiently large specimen–film distance. If necessary, however, it is possible to correct for the finite cross-section of the crystal (Hirsch, 1950). By using this method it is possible to obtain quantitative estimates of the perfection of the diffracting particles inside a polycrystalline matrix from simple back-reflexion photographs. The results on polycrystalline aluminium reported here will be interpreted, in terms of the distortion and shape of the particles, in a later paper.

The writer is indebted to Professor Sir Lawrence Bragg and Dr W. H. Taylor for suggesting the experiments and for their constant help and encouragement, and would like to record his appreciation of valuable guidance received from the late J. N. Kellar, with whom the problem was often discussed. Thanks are also due to P. Gay and Dr J. S. Thorp for their valuable help and criticism. The work was carried out during the tenure of maintenance grants from the British Iron and Steel Research Association and the Department of Scientific and Industrial Research.

References

Compton, A. H. & Allison, S. K. (1935). *X-rays in Theory and Experiment*. New York: van Nostrand.
Hirsch, P. B., & Kellar, J. N. (1952). *Acta Cryst.* **5**, 162.
Hirsch, P. B. (1950). Ph.D. Dissertation, University of Cambridge.
James, R. W. (1948). *The Optical Principles of the Diffraction of X-rays*. London: Bell.
Jones, F. W. (1938). *Proc. Roy. Soc.* A, **166**, 16.

Acta Cryst. (1952). **5**, 172

A Study of Cold-Worked Aluminium by an X-ray Micro-Beam Technique. III. The Structure of Cold-Worked Aluminium

By P. B. Hirsch

Crystallographic Laboratory, Cavendish Laboratory, Cambridge, England

(*Received* 16 *May* 1951)

The results reported in two previous papers are discussed in the light of present theories of plastic deformation of metals. It is estimated that there are $\sim 10^{10}$ dislocations/cm.^{2} in the boundaries between particles in cold-worked aluminium. The physical broadenings of the X-ray reflexions from the particles are discussed, and it is concluded that the particles are distorted. Some deductions are made about the possible types of distortion in the particles. The formation of particles is considered to be due to polygonization. The changes which occur during recovery and those induced by impurities are interpreted on this basis.

Introduction

Theories of the strength of cold-worked metals depend critically on the assumed distribution of dislocations inside the metal, but so far it has not been possible to determine this distribution experimentally. The results of the micro-beam experiments on cold-worked aluminium, however, lead to some conclusions about the possible distribution of dislocations in this metal.